CHEMISTRY OF MATERIALS

Article

pubs.acs.org/cm

Synthesis of a New Ladder-Type Benzodi(cyclopentadithiophene) Arene with Forced Planarization Leading to an Enhanced Efficiency of Organic Photovoltaics

Yung-Lung Chen, Chih-Yu Chang, Yen-Ju Cheng,* and Chain-Shu Hsu*

Department of Applied Chemistry, National Chiao Tung University, 1001 Ta Hsueh Road, Hsin-Chu, 30010 Taiwan

Supporting Information

ABSTRACT: We have developed a new heptacyclic benzodi(cyclopentadithiophene) (**BDCPDT**) unit, where 3,7-positions of the central benzo[1,2-*b*:4,5-*b*′]dithiophenes (**BDT**) subunit are covalently rigidified with 3-positons of the two external thiophenes by two carbon bridges, forming two external **CPDT** rings that share two thiophene rings with the central **BDT** core. The distannyl-**BDCPDT** building block was copolymerized with 1,3-dibromo-thieno[3,4-*c*]pyrrole-4,6-dione (**TPD**) by Stille polymerization to afford a new alternating donor−acceptor copolymer **PBDCPDT-TPD**. The implementation of forced planarization greatly suppresses the interannular twisting to extend the effective conjugated length and preserve the interactions between the donor and acceptor segments. The device using the **PBDCPDT-TPD**/$PC_{71}BM$ (1:3 in wt%) blend processed with dimethyl sulfoxide as an additive delivered a marked PCE of 6.6% which represents a significant enhancement compared to the device using the corresponding nonfused polymer analogue with a PCE of 0.2%.

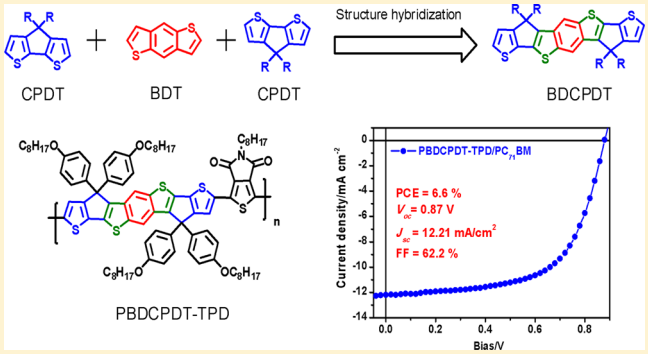

KEYWORDS: *forced planarization, conjugated polymers, solar cells, additive*

INTRODUCTION

Considerable progress has been made on the development of organic materials for photovoltaic applications in recent years.[1] Bulk heterojunction (BHJ) using an n-type and a p-type semiconductor materials in the active layer is the most widely adopted device architecture to ensure maximum internal donor−acceptor (D−A) interfacial area for efficient charge separation.[2] To achieve high efficiency of PSCs, the most critical challenge at the molecular level is to develop a p-type conjugated polymer that can simultaneously possess sufficient solubility for processability and miscibility with an n-type material low band gap (LBG) for strong and broad absorption spectrum to capture more solar photons and high hole mobility for efficient charge transport. 4*H*-Cyclopenta[2,1-*b*:3,4-*b*′]-dithiophene (**CPDT**) has attracted considerable research interest because it can act as an excellent building block to construct LBG polymers.[3] Poly[cyclopentadithiophene)-*alt*-4,7-(2,1,3-benzothiadiazole)] (**PCPDTBT**) represents one of the early successful LBG polymers for the use in PSCs.[4] The abilities to lower HOMO−LUMO energy band gap and enhance charge mobility are the advantageous features of the coplanar **CPDT** moieties. The electron-rich benzo[1,2-*b*:4,5-*b*′]dithiophene (**BDT**) derivatives, a central benzene ring fused with two thiophenes, are an attractive building block due to its symmetric, rigid, and coplanar structure. These structural characteristics are crucial to induce strong intermolecular $\pi-\pi$ interaction for efficient charge transport. Conjugated polymers incorporating benzo[1,2-*b*:4,5-*b*′]dithiophenes (**BDT**) derivatives have accomplished high-performance polymer solar cells.[5] On the other hand, thieno[3,4-*c*]pyrrole-4,6-dione (**TPD**) emerges as an unique acceptor because of its compact thoiphene-based structure with a moderate electron-withdrawing ability.[6] In 2010, Leclerc et al. first reported the synthesis of a poly(benzo[1,2-*b*:4,5-*b*′]dithiophenes-*alt*-thieno-[3,4-*c*]pyrrole 4,6-dione) **PBDT-TPD** copolymer. The solar cell with this polymer reached a high power conversion efficiency of 5.5% (Scheme 1).[7] Meanwhile, Jen et al.[8] and Fréchet et al.[9] also independently reported the **PBDT-TPD** derivatives with similar device results. In an attempt to further optimize light-harvesting and charge transporting abilities, two additional 3-octylthiophene units were introduced to the two sides of the **BDT** cores in the backbone of **PBDT-TPD**.[10] Unfortunately, the resulting polymer, poly(dithienyl **BDT**-*alt*-**TPD**) (**PDTBDT-TPD**), only yielded an unexpectedly low PCE of 0.2% (Scheme 1).[10] The dramatic decay of the performance might be attributed to the steric hindrance that severely causes the interannular twisting along the conjugated backbone of **PDTBDT-TPD**.[11] A straightforward strategy to

Received: July 30, 2012
Revised: September 13, 2012
Published: September 13, 2012

Scheme 1. Chemical Structures of PBDT-TPD, PDTBDT-TPD, and PBDCPDT-TPD

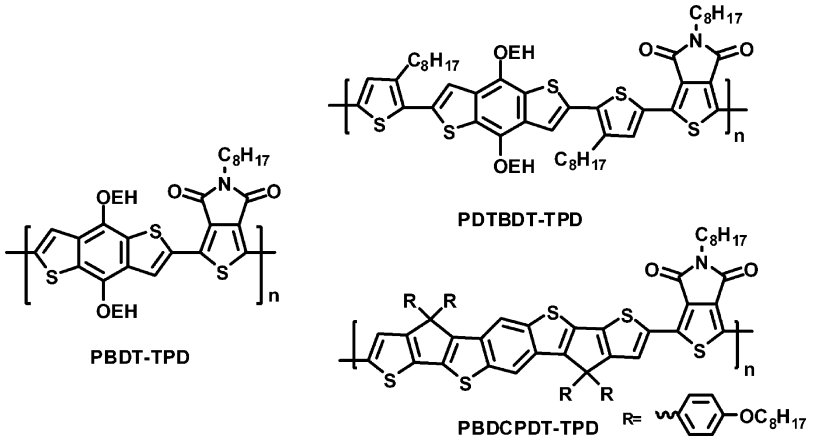

Scheme 2. Synthetic Route of the Sn-BDCPDT Monomer Leading to the Targeted PBDCPDT-TPD copolymer

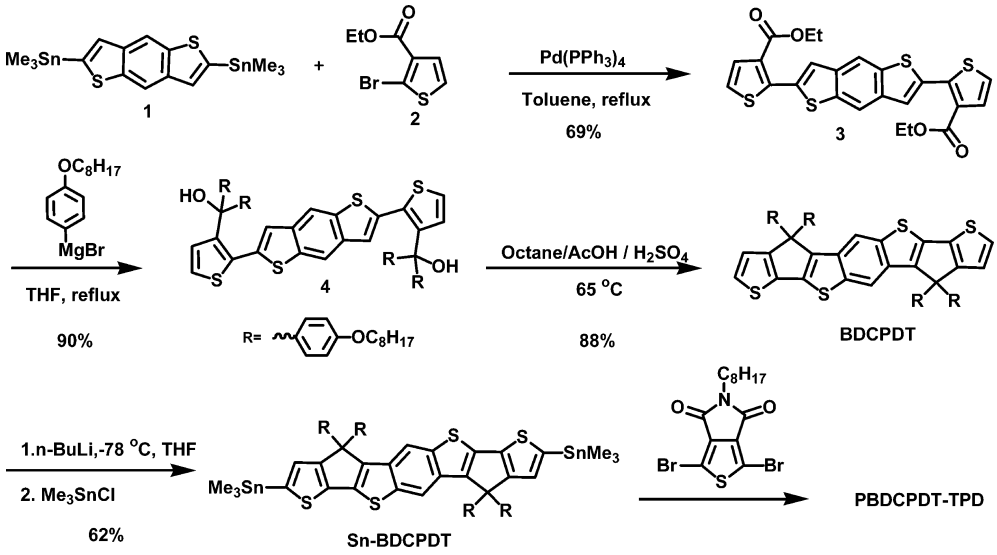

circumvent this structural deficiency is forced planarization by covalently fastening adjacent aromatic units in the polymer backbone, which strengthens the parallel p-orbital interactions to elongate effective conjugation length and facilitate intrinsic charge mobility.[12]

In this research, we have designed a new heptacyclic benzodi(cyclopentadithiophene) (**BDCPDT**) unit, where 3,7-positions of the central **BDT** subunit are covalently bridged with 3-positons of the two outer thiophenes by two carbon atoms. The ladder-type **BDCPDT** structure contains two external **CPDT** rings that share the two thiophene rings with the central **BDT** core. The **BDCPDT** unit was copolymerized with **TPD** unit to create a new alternating copolymer **PBDCPDT-TPD** (Scheme 1). In fact, **PDTBDT-TPD** and **PBDCPDT-TPD** have similar structural composition and arrangement of the conjugated backbones. The major difference is that the **BDCPDT** unit in **PBDCPDT-TPD** is covalently planarized, whereas the dithienyl-**BDT** segment in **PDTBDT-TPD** is a nonfused open-chain counterpart. This structural variation provides a good model to investigate the planarization/rigidification effect. It is anticipated that this new **CPDT**/**BDT** hybridized structure may inherit the intrinsic advantages from the **CPDT** and **BDT** moieties leading to promising electronic and optical properties attributable to a more planar and expanded conjugated structure. Furthermore, four aliphatic side chains at the two bridging carbons can readily provide sufficient solubility. As such, introducing aliphatic side chains at 4, 8 positions of the **BDT** core of **BDCPDT** is not necessary and can be thus omitted for better synthetic economy.

RESULTS AND DISCUSSION

Synthesis and Characterization. The synthetic route of **BDCPDT** is depicted in Scheme 2. Stille coupling of 2,6-trimethylstannyl **BDT** (**1**)[13] with ethyl 2-bromothiophene-3-carboxylate (**2**) yielded compound **3**. Double nucleophilic addition of the ester groups in **3** by (4-octyloxy)phenyl magnesium bromide led to the formation of benzylic alcohols in **4** which was subjected to intramolecular Friedel−Crafts cyclization under acidic condition to successfully furnish the heptacyclic arene **BDCPDT**. It should be noted that conventional preparation of the tricyclic **CPDT** unit generally requires tedious multistep synthesis.[14] Due to the ring strain, the formation of **CPDT** derivatives by using Friedel−Crafts cyclization is also not successful with low chemical yield.[15] Encouragingly, in our system, we are able to construct two **CPDT** rings in **BDCPDT** with an excellent yield of 88%. To preserve aromaticity of the central benzene ring, 3,7-positions

dx.doi.org/10.1021/cm3024082 | Chem. Mater. 2012, 24, 3964−3971

Table 1. Summary of the Intrinsic Properties of the PBDCPDT-TPD

polymer	M_n (kDa)	PDI	T_d (°C)	E_g^{opt} (eV) (film)	λ_{max} (nm) toluene	λ_{max} (nm) film	HOMO (eV)	LUMO (eV)
PBDCPDT-TPD	24.5	3.06	410	1.88	634	645	−5.36	−3.20

of the benzodithiophene core intrinsically have stronger nucleophilicity, thereby facilitating intramolecular electrophilic aromatic substitution. Afterward, the **BDCPDT** unit can be lithiated by *n*-butyllithium followed by quenching with trimethyltin chloride to afford distannyl **Sn-BDCPDT** in a moderate yield of 62%. **Sn-BDCPDT** monomer was then polymerized with 1,3-dibromo-thieno[3,4-*c*]pyrrole-4,6-dione acceptor by Stille coupling to afford a highly soluble **PBDCPDT-TPD** (M_n = 24.5 kDa, PDI = 3.06) (Scheme 2, Table 1).

Thermal Properties. The thermal stability of the polymers was analyzed by thermogravimetric analysis (TGA). It should be noted that the fused **PBDCPDT-TPD** showed much higher decomposition temperatures (T_d) of 410 °C (Figure 1) than

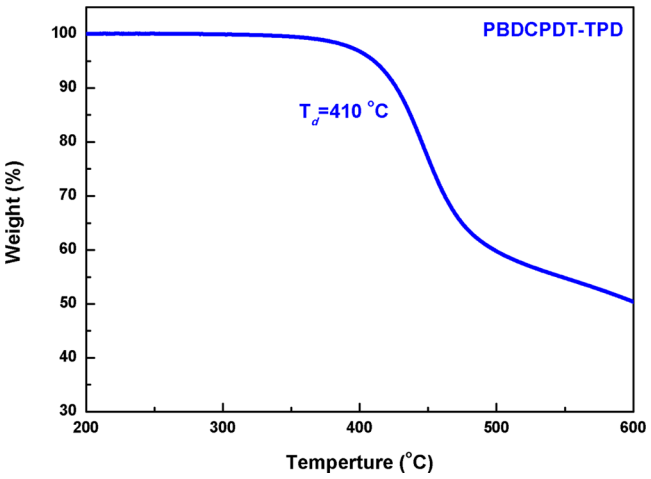

Figure 1. Thermogravimetric analysis of **PBDCPDT-TPD**.

the nonfused **PDTBDT-TPD** with T_d of 330 °C.[10] It has been proposed that dialkoxy groups at the 4, 8-positions of **BDT** units are the relatively weak sites to undergo thermal decomposition.[16] Consistently, the absence of 4, 8-substituents on the **BDT** core in our molecular design indeed improves the thermal stability of **PBDCPDT-TPD**. Thermal properties of the polymers were determined by differential scanning calorimetry (DSC). **PBDCPDT-TPD** showed neither glass transition temperatures (T_g) nor melting point, suggesting that these polymers tend to form amorphous glasses.

Optical and Electrochemical Properties. In contrast to **PBDTTPD**'s absorption spectrum showing a λ_{max} at 614 nm with vibronic structures, **PDTBDT-TPD** having two more thiophene rings in the repeating unit exhibited a single broad band with an unexpected blue-shifted λ_{max} at 517 nm.[10] The ca. 100 nm hypsochromic shift of the λ_{max} implies that the alkylthiophene rings cause steric hindrance to the central **BDT** cores, giving rise to large twisting dihedral angles around the interannular single bonds. Such disorder twisting conformations will in turn weaken the orbital interactions between the electron-rich segments and electron-deficient **TPD** units. However, with implementation of the forced planarization, **PBDCPDT-TPD** does display much red-shifted λ_{max} at 634 nm in toluene solution (Table 1). Moreover, a vibronic shoulder in its absorption spectrum reflecting rigid and coplanar characteristics of **BDCPDT** was observed again (Figure 2). Although the

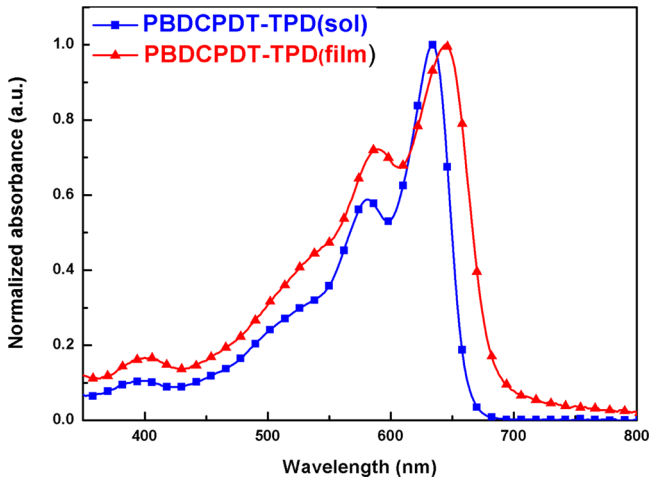

Figure 2. Normalized absorption spectra of **PBDCPDT-TPD** in toluene solution and in solid state.

profiles are essentially unchanged, the absorption spectrum of **PBDCPDT-TPD** shifts toward longer wavelengths from the solution state to the solid state, indicating that the planar structure of **BDCPDT** is capable of inducing strong interchain $\pi-\pi^*$ interactions.

Cyclic voltammetry (CV) was employed to examine the electrochemical properties (Figure 3). **PBDCPDT-TPD** showed stable and reversible p-doping/n-doping process in the cathodic and anodic scans, and a deep-lying HOMO energy level of −5.36 eV was estimated, which is at the ideal range to

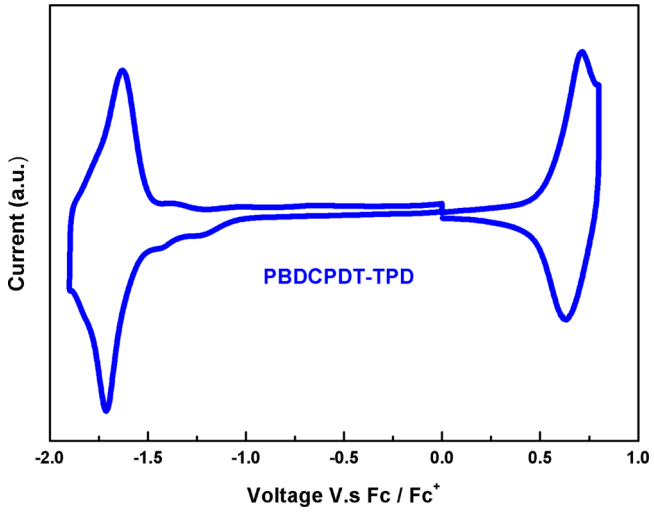

Figure 3. Cyclic voltammogram of **PBDCPDT-TPD** in the thin film at a scan rate of 100 mV/s.

dx.doi.org/10.1021/cm3024082 | *Chem. Mater.* 2012, 24, 3964−3971

ensure better air stability and greater attainable V_{oc} in the device. The LUMO energy level was determined to be −3.2 eV.

Photovoltaic and OFET Characteristics. Bulk heterojunction photovoltaic cells were fabricated on the basis of ITO/PEDOT:PSS/**PBDCPDT-TPD**:$PC_{71}BM$/Ca/Al configuration, and their performances were measured under a simulated AM 1.5 G illumination of 100 mW/cm^2. The characterization data are summarized in Table 2, and the $J-V$ curves of these

Table 2. Photovoltaic Performances of the Devices

copolymers	V_{oc} (V)	J_{sc} (mA/cm^2)	FF (%)	PCE (%)
PDTBDT-TPD[a]	0.66	1.2	26	0.2
PBDCPDT-TPD[b]	0.85	11.71	51.7	5.1
PBDCPDT-TPD[c]	0.85	11.95	60.4	6.1
PBDCPDT-TPD[d]	0.87	12.21	62.2	6.6

[a]Data reported from ref 10. [b]Device A: ITO/PEDOT:PSS/**PBDCPDT-TPD**:$PC_{71}BM$ (1:3 in wt %)/Ca/Al. [c]Device B: ITO/PEDOT:PSS/**PBDCPDT-TPD**:$PC_{71}BM$ (1:3 in wt %) with DMSO/Ca/Al. [d]Device C: ITO/MoO_3/**PBDCPDT-TPD**:$PC_{71}BM$ (1:3 in wt %) with DMSO/Ca/Al.

polymers are shown in Figure 4. The device A using **PBDCPDT-TPD**:$PC_{71}BM$ (1:3 in wt %) showed a high PCE of 5.1% with a V_{oc} of 0.85 V, a J_{sc} of 11.71 cm^2 V^{-1} s^{-1}, and a FF of 51.7%. In sharp contrast, the device incorporating nonfused **PDTBDT-TPD** counterpart only achieved a low PCE of 0.2% with a V_{oc} of 0.66 V, a J_{sc} of 1.2 cm^2 V^{-1} s^{-1}, and a FF of 26%.[10] Clearly, twisting of the conjugated backbone of **PDTBDT-TPD** severely affects the charge transporting properties. Nanoscale morphology of the active layer can be controlled and optimized by judicial choice of the processing additives.[17] We envision that polar dimethylsulfoxide (DMSO) can serve as a good alternative for a binary polymer:$PC_{71}BM$ blending system.[18] First, the boiling point of DMSO is higher than that of the host solvent of *ortho*-dichlorobenzene (ODCB). Second, DMSO is a good solvent for the $PC_{71}BM$ component but a relatively poor solvent for the **PBDCPDT-TPD** polymer. Therefore, the presence of a small amount of DMSO may induce a closer intermolecular packing of **PBDCPDT-TPD**. Encouragingly, by adding 5 vol % DMSO into ODCB as the processing additive in device B, the PCE was improved to 6.1% with a V_{oc} of 0.85, a J_{sc} of 11.95 cm^2 V^{-1} s^{-1}, and a FF of 60.4%. Compared to the nonadditive device, the device processed with DMSO additive exhibited a pronounced enhancement of incident photon to current efficiency (IPCE) from 570 to 700 nm of light illumination, which is highly associated with **PBDCPDT-TPD**'s improved absorption ability (Figure 4). To gain more insight into the performance enhancement upon the introduction of DMSO additive, the morphology of the blend films was investigated by atomic force microscope (AFM) (Figure 5). Compared to the pristine film, the additive-processed **PBDCPDT-TPD**:$PC_{71}BM$ film indeed showed larger surface roughness presumably due to the higher degree of **PBDCPDT-TPD** aggregation, resulting in more favorable morphological phase separation for efficient charge separation and transport. The morphological changes induced by the DMSO additive were consistent with the hole mobility (u_h) estimated from space-charge-limited current (SCLC) and field-effect transistor (FET) measurements, as shown in Table 3. The SCLC hole mobility of the additive-processed device reached 2.5 × 10^{-3} cm^2 V^{-1} s^{-1}, which is more than 1 order of magnitude higher than that of the nonadditive device (4.0 × 10^{-4} cm^2 V^{-1} s^{-1}). In addition, a slightly higher FET hole mobility (6.8 × 10^{-2} cm^2 V^{-1} s^{-1}) was also observed in the additive-processed device as compared with that of the nonadditive device (5.6 × 10^{-2} cm^2 V^{-1} s^{-1}) (Figure 6).

Furthermore, by changing the hole-extraction layer from PEDOT:PSS to a layer of MoO_3 in device C,[19] all the parameters were further improved, leading to a highest efficiency of 6.6% with a V_{oc} of 0.87 V, a J_{sc} of 12.21 cm^2 V^{-1} s^{-1}, and a FF of 62.2%. It has been known that the work function of MoO_3 is located at −5.4 eV.[19] The enhancement may be ascribed to the close energy alignment between the work function of MoO_3 and the HOMO energy level of **PBDCPDT-TPD**, thereby facilitating charge transporting at the interface.

CONCLUSIONS

We have developed a new ladder-type **BDCPDT** unit integrating the well-known **CPDT** and **BDT** subunits into a coplanar conjugated entity. By taking advantage of the stronger nucleophilicity at the 3,7-positions of the **BDT** unit, **BDCPDT** arene can be successfully synthesized with a high yield through a Friedel−Crafts cyclization. Due to the coplanar, symmetrical, and elongated conjugated structure of **BDCPDT**, strong donor−acceptor interactions along the conjugated backbone can be preserved, leading to more red-shifted and broader absorption spectrum and better charge mobility. Under the optimal device conditions using DMSO as the additive and MoO_3 as the hole-selective layer, the device using **PBDCPDT-**

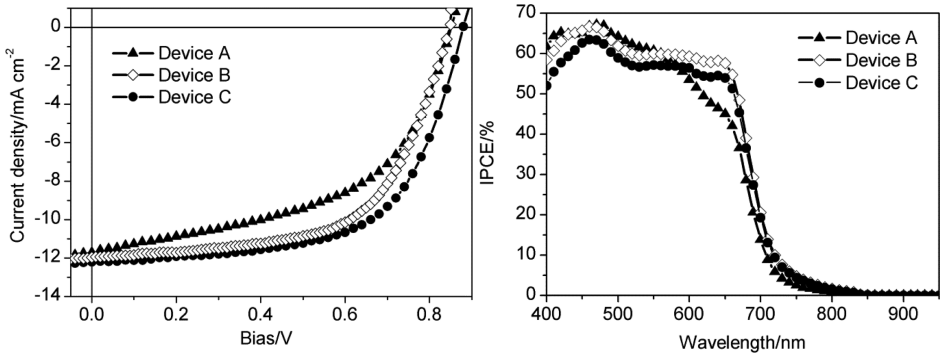

Figure 4. Current density−voltage characteristics (left) and IPCE spectra (right) of the devices. Device A: ITO/PEDOT:PSS/**PBDCPDT-TPD**:$PC_{71}BM$ (1:3 in wt %)/Ca/Al); device B: ITO/PEDOT:PSS/**PBDCPDT-TPD**:$PC_{71}BM$ (1:3 in wt %) with DMSO/Ca/Al); device C: ITO/MoO_3/**PBDCPDT-TPD**:$PC_{71}BM$ (1:3 in wt %) with DMSO/Ca/Al).

dx.doi.org/10.1021/cm3024082 | *Chem. Mater.* 2012, 24, 3964−3971

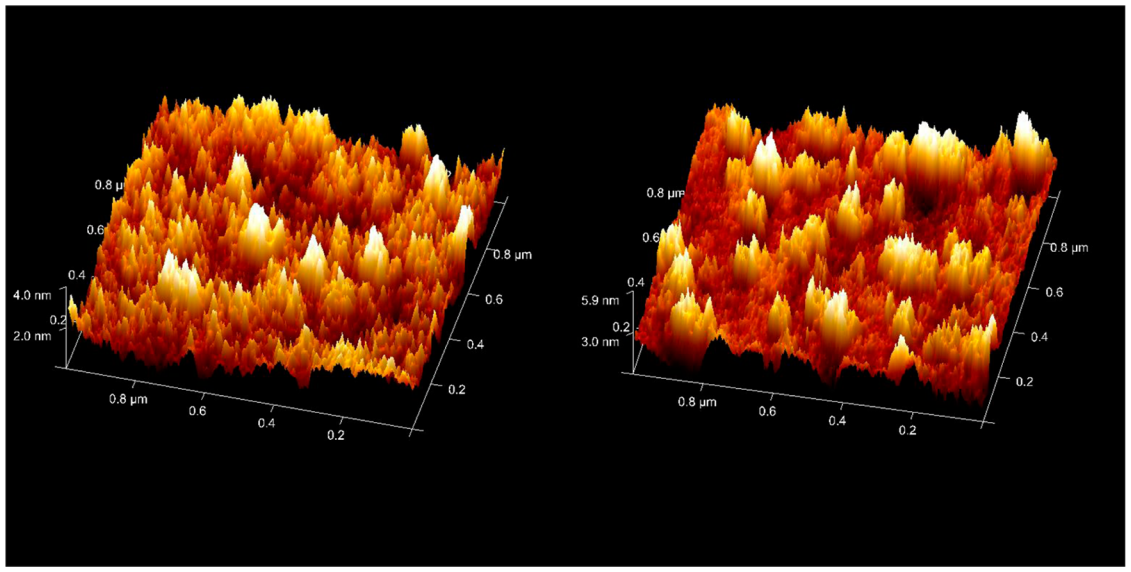

Figure 5. AFM tapping mode height images of the surface of **PBDCPDT-TPD**/$PC_{71}BM$ (left) and **PBDCPDT-TPD**/$PC_{71}BM$ with 5 vol % DMSO (right) (1.0 μm × 1.0 μm).

Table 3. SCLC and FET Hole Mobilities of the Device Processed with and without DMSO Additive

condition	u_h ($cm^2\ V^{-1}\ s^{-1}$)
no additive, SCLC	4.0×10^{-4}
with additive, SCLC	2.5×10^{-3}
no additive, FET	5.6×10^{-2}
with additive, FET	6.8×10^{-2}

TPD:$PC_{71}BM$ (1:3 in wt %) has delivered a marked PCE of 6.6%, which is one of the best performances among the **BDT**-based or **TPD**-based copolymers. This efficiency dramatically outperforms the device using the corresponding nonfused **PDTBDT-TPD** as the donor material.

■ EXPERIMENTAL SECTION

All chemicals are purchased from Aldrich or Acros and used as received unless otherwise specified. ^1H and ^{13}C NMR spectra were measured using a Varian 300 MHz instrument spectrometer. Differential scanning calorimetery (DSC) was measured on a TA Q200 Instrument, and thermogravimetric analysis (TGA) was recorded on a Perkin-Elmer Pyris under nitrogen atmosphere at a heating rate of 10 °C/min. Absorption spectra were collected on a HP8453 UV−vis spectrophotometer. The molecular weights of polymers were measured by the GPC method on a Viscotek VE2001GPC, and polystyrene was used as the standard (THF as the eluent). The electrochemical cyclic voltammetry (CV) was conducted on a Autolab ADC 164. A glassy carbon electrode coated with a thin polymer film was used as the working electrode and standard calomel electrode as the reference electrode, while 0.1 M tetrabutylammonium tetrafluoroborate (Bu_4NBF_4) in acetonitrile was the electrolyte. CV curves were calibrated using ferrocence as the standard, whose oxidation potential is set at −4.8 eV with respect to zero vacuum level. The HOMO energy levels were obtained from the equation HOMO = $-e(E_{ox}^{onset} - E_{(ferrocene)}^{onset} + 4.8)$ eV. The LUMO levels of polymer were obtained from the equation LUMO = $-e(E_{red}^{onset} - E_{(ferrocene)}^{onset} + 4.8)$ eV. Surface topography was investigated using Veeco Nanoscope 3100 AFM and standard tips (type Tap 300; L, 135 m; FREQ, 300 MHz; k, 40 N/m).

Solar Cell Device Fabrication. ITO/Glass substrates were ultrasonically cleaned sequentially in detergent, water, acetone, and isopropyl alcohol. Then, the substrates were covered by either a 30 nm PEDOT:PSS (Clevios 4083 provided by H. C. Stark) or a 10 nm thermally evaporated MoO_3 as the hole-extraction layer. After annealing in air at 150 °C during 30 min, the samples were cooled down to rt. The active layer (90 nm thick) consisting of the blend of **PBDCPDT-TPD** and $PC_{71}BM$ (Nano C) with a weight ratio of 1:3 (with or without 5 vol % DMSO) was then spin coated from *ortho*-dichlorobenzene (ODCB) solvent. After annealing the active layer at 150 °C for 10 min, the cathode made of calcium (25 nm thick) and aluminum (100 nm thick) was evaporated through a shadow mask under high vacuum ($<10^{-6}$ Torr). Each device is constituted of four pixels defined by an active area of 0.04 cm^2. The current density−voltage (J−V) characteristics were measured under simulated air mass 1.5 global (AM 1.5G) irradiation of 100 mW cm^{-2}.

Hole-Only Devices. In order to investigate the respective hole mobility of the different copolymer films, unipolar devices have been prepared following the same procedure except that the active layer is made of pure **PBDCPDT-TPD** and the Ca/Al cathode is replaced by evaporated gold (40 nm). The hole mobilities were calculated according to space charge limited current theory (SCLC). The J−V curves were fitted according to the following equation:

$$J = \frac{9}{8}\varepsilon\mu\frac{V^2}{L^3}$$

where ε is the dielectric permittivity of the **PBDCPDT-TPD**, μ is the hole mobility, and L is the film thickness (distance between the two electrodes)

FET Device Fabrication. An n-type heavily doped Si wafer with a SiO_2 layer of 300 nm and a capacitance of 11 nF cm^{-2} was used as the gate electrode and dielectric layer. Thin films (40−60 nm in thickness) of **PBDCPDT-TPD** were deposited on octadecantrichlorosilane (OTS)-treated SiO_2/Si substrates by spin-coating their *o*-dichlorobenzene solutions (6 mg mL^{-1}). Then, the thin films were annealed at 150 °C for 10 min. Gold source and drain contacts (60 nm thick) were deposited by vacuum evaporation on the active layer through a shadow mask, affording a bottom-gate, top-contact device configuration. Electrical measurements of OTFT devices were carried out at room temperature in air using a 4156C (Agilent Technologies). The field-effect mobility was calculated in the saturation regime by using the equation $I_{DS} = (\mu WC_i/2L)(V_G - V_T)^2$, where I_{DS} is the drain-source current, μ is the field-effect mobility, W is the channel width (3500 μm), L is the channel length (60 μm), C_i is the capacitance per unit area of the gate dielectric layer, and V_G is the gate voltage.

Synthesis of Compound 3. To a 100 mL round-bottom flask was introduced **1** (2 g, 3.88 mmol), ethyl 2-bromothiophene-3-carboxylate **2** (2.81 g, 9.31 mmol), $Pd(PPh_3)_4$ (0.22 g, 0.19 mmol), and degassed

dx.doi.org/10.1021/cm3024082 | *Chem. Mater.* 2012, 24, 3964−3971

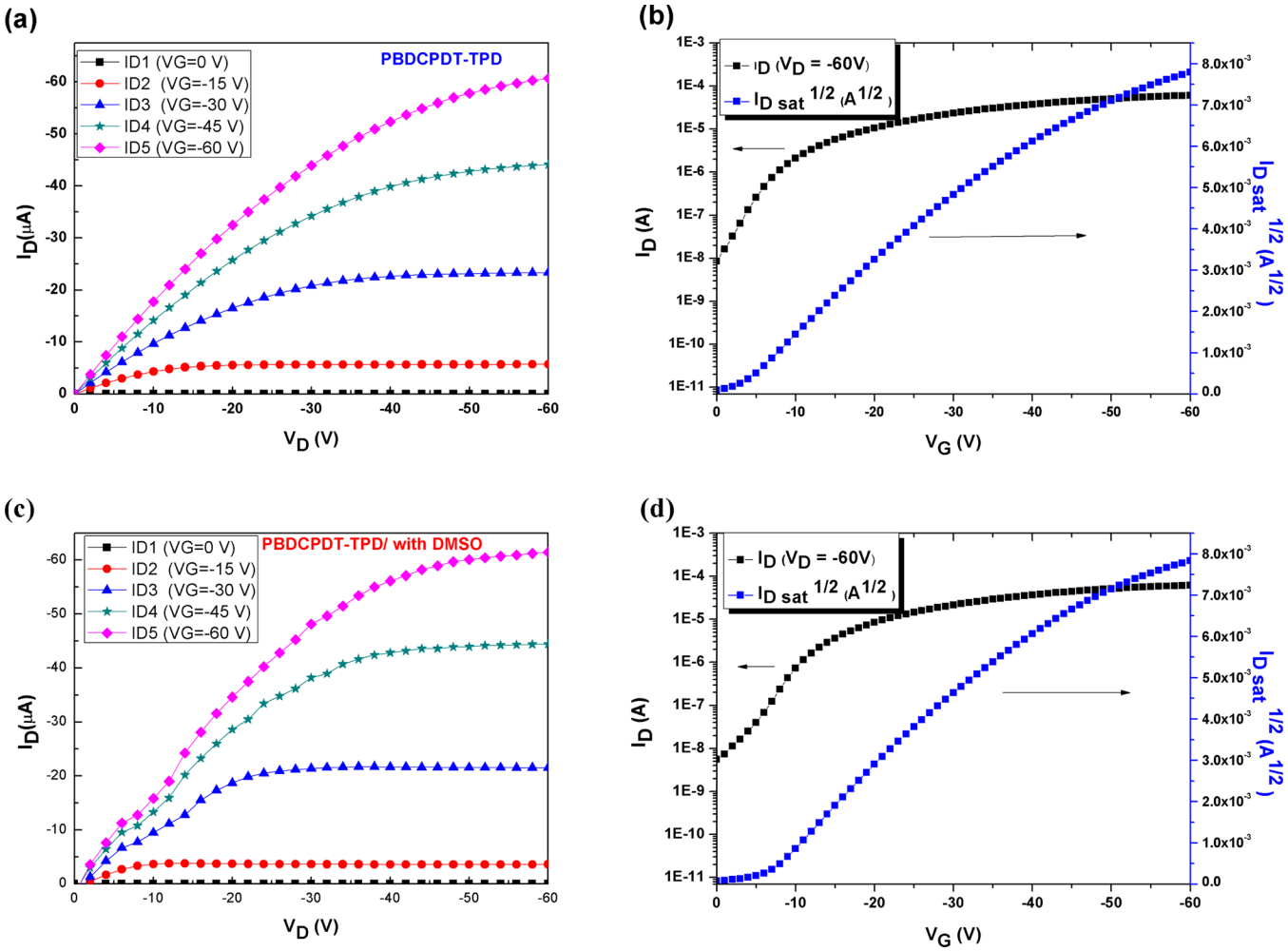

Figure 6. Output characteristics of p-type OFET devices of **PBDCPDT-TPD** (a, b) and **PBDCPDT-TPD** with 5 vol % DMSO (c, d).

toluene (40 mL). The mixture was heated to reflux under nitrogen for 16 h. After removal of toluene under reduced pressure, the residue was purified by column chromatography on silica gel (hexane/ethyl acetate, v/v, 10/1) and then recrystallized from THF to give an orange solid **3** (1.34 g, 69%). ^{1}H NMR ($CDCl_3$, 300 MHz, ppm): δ 1.31 (t, J = 7.2 Hz, 6 H), 4.33 (q, J = 7.2 Hz, 4H), 7.29 (d, J = 5.4 Hz, 2 H), 7.55 (d, J = 5.4 Hz, 2 H), 7.75 (s, 2 H), 8.21 (s, 2 H). ^{13}C NMR ($CDCl_3$, 75 MHz, ppm): δ 14.4, 61.1, 116.9, 125.1, 129.4, 130.9, 135.1, 138.1, 138.3, 142.7, 158.0, 163.2. MS (EI, $C_{24}H_{18}O_4S_4$): calcd, 498.66; found, 498.

Synthesis of Compound 4. A Grignard reagent was prepared by the following procedure. To a suspension of magnesium turnings (0.36 g, 15.0 mmol) and 3–4 drops of 1,2-dibromoethane in dry THF (10 mL) was slowly added 1-bromo-4-(octyloxy)benzene (4.02 g, 15.0 mmol) dropwise, and the mixture was stirred for 1 h. To a solution of **3** (0.5 g, 1 mmol) in dry THF (40 mL) under nitrogen was added 4-(octyloxy)benzene 1-magnesium bromide (5 mL, 5 mmol) dropwise at room temperature. The resulting mixture was heated at reflux for 16 h. The reaction solution was extracted with diethyl ether (50 mL × 3) and ammonium chloride solution (150 mL). The combined organic layer was dried over $MgSO_4$. After removal of the solvent under reduced pressure, the residue was purified by column chromatography on silica gel (hexane/ethyl acetate, v/v, 10/1) to give a brown oil **4** (1.15 g, 93%). ^{1}H NMR ($CDCl_3$, 300 MHz, ppm): δ 0.89 (t, J = 6.3 Hz, 12 H), 1.30–1.46 (m, 40 H), 1.75–1.80 (m, 8 H), 3.44 (s, 2 H), 3.93 (t, J = 6.6 Hz, 8 H), 6.45 (d, J = 5.4 Hz, 2 H), 6.82 (d, J = 7.8 Hz, 8 H), 6.88 (s, 2 H), 7.158 (d, J = 7.8 Hz, 8 H), 7.162 (d, J = 5.4 Hz, 2 H), 7.87 (s, 2 H). ^{13}C NMR ($CDCl_3$, 75 MHz, ppm): δ 14.4, 23.0, 26.3, 29.6, 29.7, 32.0, 68.2, 80.4, 114.0, 116.6, 124.4, 124.5, 129.1, 131.8, 132.1, 136.9, 137.7, 138.1, 140.0, 146.9, 158.6. MS (FAB, $C_{76}H_{94}O_6S_4$): calcd, 1231.82; found, 1230.

Synthesis of BDCPDT. To a solution of **4** (1 g, 0.8 mmol) in octane (100 mL) was added acetic acid (10 mL) and sulfuric acid (1 mL, 19 mmol) slowly. The resulting solution was stirred for 4 h at 65 °C. After removal of the octane under reduced pressure, the residue was extracted by sodium carbonate solution (50 mL × 3) and diethyl ether (50 mL × 2) . Then, the crude products were purified by column chromatography on silica gel (hexane/ethyl acetate, v/v, 100/1) to give a yellow oil **BDCPDT** (0.85 g, 88%). ^{1}H NMR ($CDCl_3$, 300 MHz, ppm): δ 0.88 (t, J = 6.9 Hz, 12 H), 1.28–1.45 (m, 40 H), 1.71–1.76 (m, 8 H), 3.88 (t, J = 6.6 Hz, 8 H), 6.77 (d, J = 8.7 Hz, 8 H), 7.07 (d, J = 4.8 Hz, 2 H), 7.17 (d, J = 8.7 Hz, 8 H), 7.25 (d, J = 4.8 Hz, 2 H), 7.88 (s, 2 H).^{13}C NMR ($CDCl_3$, 75 MHz, ppm): 14.4, 22.9, 26.3, 29.5, 29.6, 32.1, 61.9, 68.1, 114.6, 116.2, 123.0, 127.2, 129.5, 131.2, 134.0, 136.7, 137.4, 141.8, 149.6, 158.4, 162.1. MS (FAB, $C_{76}H_{90}O_4S_4$): calcd, 1195.79; found, 1195.

Synthesis of Sn-BDCPDT. To a solution of **BDCPDT** (0.45 g, 0.38 mmol) in dry THF (15 mL) was added a 2.5 M solution of *n*-BuLi in hexane (0.4 mL, 1 mmol) dropwise at −78 °C. After stirring at −78 °C for 30 min and at RT for 30 min, a 1.0 M solution of chlorotrimethylstannane in THF (1.14 mL, 1.14 mmol) was introduced by syringe to the solution at −78 °C. The mixture solution was quenched with water and extracted with diethyl ether (50 mL × 2) and water (50 mL). The combined organic layer was dried over $MgSO_4$. After removal of the solvent under reduced pressure, the residue was purified by recrystallizing from hexane to give a yellow solid **Sn-BDCPDT** (382 mg, 62%). ^{1}H NMR ($CDCl_3$, 300 MHz, ppm): δ 0.36 (s, 18 H), 0.88 (t, J = 6 Hz, 12 H), 1.28–1.43 (m, 40 H),

dx.doi.org/10.1021/cm3024082 | Chem. Mater. 2012, 24, 3964–3971

1.70−1.74 (m, 8 H), 3.88 (t, J = 6.6 Hz, 8 H), 6.76 (d, J = 9 Hz, 8 H), 7.07 (s, 2 H), 7.17 (d, J = 9 Hz, 8 H), 7.82 (s, 2 H). ^{13}C NMR ($CDCl_3$, 75 MHz, ppm): δ −7.74, 14.3, 22.9, 26.3, 29.45, 29.51, 29.6, 32.0, 61.3, 68.1, 114.5, 116.1, 129.6, 130.2, 131.3, 134.3, 137.4, 141.1, 141.7, 142.5, 149.4, 158.3, 164.0. MS (FAB, $C_{82}H_{106}O_4S_4Sn_2$): calcd, 1521.4; found, 1521.

Synthesis of PBDCPDT-TPD via Microwave-Assisted Stille Coupling Polymerization. To a 50 mL round-bottom flask was introduced **Sn-BDCPDT** (180 mg, 0.118 mmol), 1,3-dibromothieno[3,4-*c*]pyrrole-4,6-dione (50 mg, 0.118 mmol), $Pd_2(dba)_3$ (4.3 mg, 0.0047 mmol), tri(*o*-tolyl)phosphine (11.5 mg, 0.037 mmol), and dry chlorobenzene (8 mL). The mixture was then degassed by bubbling nitrogen for 10 min at room temperature. The round-bottom flask was placed into the microwave reactor and reacted for 50 min under 270 W. To end-cap the resulting polymer, tributyl(thiophen-2-yl)stannane (22.3 mg, 0.059 mmol) was added to the mixture solution and reacted for 10 min under 270 W. Finally, 2-bromothiophene (9.61 mg, 0.063 mmol) was added to the mixture solution and reacted for 10 min under 270 W. The solution was added into methanol dropwise. The precipitate was collected by filtration and washed by Soxhlet extraction with acetone and hexane sequentially for three days. The polymer was dissolved in hot THF, and the residual Pd catalyst and Sn metal in THF solution was removed by Pd-thiol gel and Pd-TAAcOH (Silicycle Inc.). After filtration and removal of the solvent, the polymer was redissolved in THF again and added into methanol to precipitate. The purified polymer was collected by filtration and dried under vacuum for 1 day to give a dark-purple fiber-like solid (140 mg, 81%, Mn = 24500, PDI = 3.06). ^{1}H NMR ($CDCl_3$, 300 MHz): δ 0.86 (br, 12 H), 1.26−1.38 (br, 40 H), 1.72 (br, 8 H), 3.88 (br, 8 H), 6.78 (br, 8 H), 7.18 (br, 8 H), 7.87 (br, 4 H).

■ ASSOCIATED CONTENT

Ⓢ Supporting Information

^{1}H and ^{13}C NMR spectra of the new compounds and **PBDCPDT-TPD** polymer. This material is available free of charge via the Internet at http://pubs.acs.org.

■ AUTHOR INFORMATION

Corresponding Author

*E-mail: yjcheng@mail.nctu.edu.tw (Y.-J.C.); cshsu@mail.nctu.edu.tw (C.-S.H.).

Notes

The authors declare no competing financial interest.

■ ACKNOWLEDGMENTS

This work is supported by the National Science Council and "ATP program" of the National Chiao Tung University and Ministry of Education, Taiwan.

■ REFERENCES

(1) (a) Thompson, B. C.; Fréchet, J. M. J. *Angew. Chem., Int. Ed.* **2008**, *47*, 58. (b) Cheng, Y.-J.; Yang, S.-H.; Hsu, C.-S. *Chem. Rev.* **2009**, *109*, 5868. (c) Chen, J.; Cao, Y. *Acc. Chem. Res.* **2009**, *42*, 1709. (d) Li, Y.; Zou, Y. *Adv. Mater.* **2008**, *20*, 2952. (e) Li, Y. *Acc. Chem. Res.* **2012**, *45*, 723. (f) Yip, H.-L.; Jen, A. K.-Y. *Energy Environ. Sci.* **2012**, *5*, 5994.

(2) Yu, G.; Gao, J.; Hummelen, J. C.; Wudl, F.; Heeger, A. J. *Science* **1995**, *270*, 1789.

(3) (a) Bijleveld, J. C.; Shahid, M.; Gilot, J.; Wienk, M. M.; Janssen, A. J. *Adv. Funct. Mater.* **2009**, *19*, 3262. (b) Tsao, H. N.; Cho, D. M.; Park, I.; Hansen, M. R.; Mavrinskiy, A.; Yoon, D. Y.; Graf, R.; Pisula, W.; Spiess, H. W.; Müllen, K. *J. Am. Chem. Soc.* **2011**, *133*, 2605. (c) Li, Z.; Tsang, S. W.; Du, X.; Scoles, L.; Robertson, G.; Zhang, Y.; Toll, F.; Tao, Y.; Lu, J.; Ding, J. *Adv. Funct. Mater.* **2011**, *21*, 3331. (d) Zhang, Y.; Zou, J.; Yip, H. L.; Sun, Y.; Davies, J. A.; Chen, K. S.; Acton, O.; Jen, A. K.Y. *J. Mater. Chem.* **2011**, *21*, 3895.

(4) (a) Peet, J.; Kim, J. Y.; Coates, N. E.; Ma, W. L.; Moses, D.; Heeger, A. J.; Bazan, G. C. *Nat. Mater.* **2007**, *6*, 497. (b) Zhu, Z.; Waller, D.; Gaudiana, R.; Morana, M.; Mühlbacher, D.; Scharber, M.; Brabec, C. *Macromolecules* **2007**, *40*, 1981.

(5) (a) Hou, J.; Chen, H.-Y.; Zhang, S.; Chen, R. I.; Yang, Y.; Wu, Y.; Li, G. *J. Am. Chem. Soc.* **2009**, *131*, 15586. (b) Zhou, H.; Yang, L.; Stuart, A. C.; Price, S. C.; Liu, S.; You, W. *Angew. Chem., Int. Ed.* **2011**, *50*, 2995. (c) Huo, L.; Hou, J. *Polym. Chem.* **2011**, *2*, 2453. (d) Son, H. J.; Wang, W.; Xu, T.; Liang, Y.; Wu, Y.; Li, G.; Yu, L. *J. Am. Chem. Soc.* **2011**, *133*, 1885. (e) Boudreault, P.-L. T.; Najari, A.; Leclerc, M. *Chem. Mater.* **2011**, *23*, 456. (f) Pan, H.; Li, Y.; Wu, Y.; Liu, P.; Ong, B. S.; Zhu, S.; Xu, G. *J. Am. Chem. Soc.* **2007**, *129*, 4112. (g) Zhang, M.; Guo, X.; Li, Y. *Macromolecules* **2011**, *44*, 8798. (h) Wang, M.; Hu, X.; Liu, P.; Li, W.; Gong, x.; Huang, F.; Cao, Y. *J. Am. Chem. Soc.* **2011**, *133*, 9638. (i) Huo, L.; Guo, X.; Zhang, S.; Li, Y.; Hou, J. *Macromolecules* **2011**, *44*, 4035.

(6) (a) Nielsen, C. B.; Bjørnholm, T. *Org. Lett.* **2004**, *6*, 3381. (b) Chen, C. M.; Amb, S.; Graham, K. R.; Subbiah, J.; Small, C. E.; So, F.; Reynolds, J. R. *J. Am. Chem. Soc.* **2011**, *133*, 10062. (c) Chu, T. Y.; Lu, J.; Beaupré, S.; Zhang, Y.; Pouliot, J. R.; Wakim, S.; Zhou, J.; Leclerc, M.; Li, Z.; Ding, J.; Tao, Y. *J. Am. Chem. Soc.* **2011**, *133*, 4250. (d) Berrouard, P.; Najari, A.; Pron, A.; Gendron, D.; Morin, P.-O.; Pouliot, J.-R.; Veilleux, J.; Leclerc, M. *Angew. Chem., Int. Ed.* **2012**, *51*, 2068.

(7) Zou, Y.; Najari, A.; Berrouard, P.; Beaupré, S.; Aïch, B. R.; Tao, Y.; Leclerc, M. *J. Am. Chem. Soc.* **2010**, *132*, 5330.

(8) Zhang, Y.; Hau, S. K.; Yip, H. L.; Sun, Y.; Acton, O.; Jen, A. K. Y. *Chem. Mater.* **2010**, *22*, 2696.

(9) Piliego, C.; Holcombe, T. W.; Douglas, J. D.; Woo, C. H.; Beaujuge, P. M.; Fréchet, J. M. J. *J. Am. Chem. Soc.* **2010**, *132*, 7595.

(10) Najari, A.; Beaupré, S.; Berrouard, P.; Zou, Y.; Pouliot, J. R.; Pérusse, C. L.; Leclerc, M. *Adv. Funct. Mater.* **2011**, *21*, 718.

(11) Zhou, H.; Yang, L.; Xiao, S.; Liu, S.; You, W. *Macromolecules* **2010**, *43*, 811.

(12) (a) Liang, Y.; Wu, Y.; Feng, D.; Tsai, S.-T.; Son, H.-J.; Li, G.; Yu, L. *J. Am. Chem. Soc.* **2009**, *131*, 56. (b) He, F.; Wang, W.; Chen, W.; Xu, T.; Darling, S. B.; Strzalka, J.; Liu, Y.; Yu, L. *J. Am. Chem. Soc.* **2011**, *133*, 3284. (c) Zhang, Y.; Zou, J.; Yip, H.-L.; Chen, K.-S.; Zeigler, D. F.; Sun, Y.; Jen, A. K.-Y. *Chem. Mater.* **2011**, *23*, 2289. (d) Cheng, Y.-J.; Wu, J.-S.; Shih, P.-I.; Chang, C.-Y.; Jwo, P.-C.; Kao, W.-S.; Hsu, C.-S. *Chem. Mater.* **2011**, *23*, 2361. (e) Wu, J.-S.; Cheng, Y.-J.; Dubosc, M.; Hsieh, C.-H.; Chang, C.-Y.; Hsu, C.-S. *Chem. Commun.* **2010**, *46*, 3259. (f) Wu, J.-S.; Cheng, Y.-J.; Lin, T.-Y.; Chang, C.-Y.; Shih, P.-I.; Hsu, C.-S. *Adv. Funct. Mater.* **2012**, *22*, 1711. (g) Wang, J.-Y.; Hau, S. K.; Yip, H.-L.; Davies, J. A.; Chen, K.-S.; Zhang, Y.; Sun, Y.; Jen, A. K.-Y. *Chem. Mater.* **2011**, *23*, 765. (h) Ashraf, R. S.; Chen, Z.; Leem, D. S.; Bronstein, H.; Zhang, W.; Schroeder, B.; Geerts, Y.; Smith, J.; Watkins, S.; Anthopoulos, T. D.; Sirringhaus, H.; Mello, J. C.; de; Heeney, M.; McCulloch, I. *Chem. Mater.* **2011**, *23*, 768. (i) Chen, C.-H.; Cheng, Y.-J.; Dubosc, M.; Hsieh, C.-H.; Chu, C.-C.; Hsu, C.-S. *Chem. Asian J.* **2010**, *5*, 2480. (j) Zhang, M.; Guo, X.; Wang, X.; Wang, H.; Li, Y. *Chem. Mater.* **2011**, *23*, 4264. (k) Cheng, Y.-J.; Chen, C.-H.; Lin, Y.-S.; Chang, C.-Y.; Hsu, C.-S. *Chem. Mater.* **2011**, *23*, 5068. (l) Chen, C.-H.; Cheng, Y.-J.; Chang, C.-Y.; Hsu, C.-S. *Macromolecules* **2011**, *44*, 8415. (m) Cheng, Y.-J.; Ho, Y.-J.; Chen, C.-H.; Kao, W.-S.; Wu, C.-E.; Hsu, S.-L.; Hsu, C.-S. *Macromolecules* **2012**, *45*, 2690. (n) Cheng, Y.-J.; Cheng, S.-W.; Chang, C.-Y.; Kao, W.-S.; Liao, M.-H.; Hsu, C.-S. *Chem. Commun.* **2012**, *48*, 3203. (o) Forster, M.; Annan, K. O.; Scherf, U. *Macromolecules* **1999**, *32*, 3159. (p) Scherf, U. *J. Mater. Chem.* **1999**, *9*, 1853. (q) Chmil, K.; Scherf, U. *Acta Polym.* **1997**, *48*, 208. (r) Chmil, K.; Scherf, U. *Makromol. Chem., Rapid Commun.* **1993**, *14*, 217. (s) Facchetti, A. *Chem. Mater.* **2011**, *23*, 733. (t) Guo, X.; Ortiz, R. P.; Zheng, Y.; Hu, Y.; Noh, Y.-Y.; Baeg, K.-J.; Facchetti, A.; Marks, T. J. *J. Am. Chem. Soc.* **2011**, *133*, 1405.

(13) Rieger, R.; Beckmann, D.; Mavrinskiy, A.; Kastler, M.; Müllen, K. *Chem. Mater.* **2010**, *22*, 5314.

(14) Chen, C. H.; Hsieh, C. H.; Dubosc, M.; Cheng, Y. J.; Hsu, C. S. *Macromolecules* **2010**, *43*, 697.

(15) (a) Mierloo, S. V.; Adriaensens, P. J.; Maes, W.; Lutsen, L.; Cleij, T. J.; Botek, E.; Champagne, B.; Vanderzande, D. J. *J. Org. Chem.* **2010**, *75*, 7202. (b) Cheng, Y. J.; Chen, C. H.; Lin, T. Y.; Hsu, C. S. *Chem. Asian J.* **2012**, *7*, 818.
(16) Huo, L.; Zhang, S.; Guo, X.; Xu, F.; Li, Y.; Hou, J. *Angew. Chem., Int. Ed.* **2011**, *50*, 9697.
(17) (a) Lee, J. K.; Ma, W. L.; Brabec, C. J.; Yuen, J.; Moon, J. S.; Kim, J. Y.; Lee, K.; Bazan, G. C.; Heeger, A. J. *J. Am. Chem. Soc.* **2008**, *130*, 3619. (b) Rogers, J. T.; Schmidt, K.; Toney, M. F.; Kramer, E. J.; Bazan, G. C. *Adv. Mater.* **2011**, *23*, 2284. (c) Chang, C.-Y.; Cheng, Y.-J.; Hung, S.-H.; Wu, J.-S.; Kao, W.-S.; Lee, C.-H.; Hsu, C.-S. *Adv. Mater.* **2012**, *24*, 549.
(18) Chu, T. Y.; Alem, S.; Tsang, S.-W.; Tse, S. C.; Wakim, S.; Lu, J.; Dennler, G.; Waller, D.; Gaudiana, R.; Tao, Y. *Appl. Phys. Lett.* **2011**, *98*, 253301.
(19) (a) Sun, Y.; Takacs, C. J.; Cowan, S. R.; Seo, J. H.; Gong, X.; Roy, A.; Heeger, A. J. *Adv. Mater.* **2011**, *23*, 2226. (b) Fan, X.; Cui, C.; Fang, G.; Wang, J.; Li, S.; Cheng, F.; Long, H.; Li, Y. *Adv. Funct. Mater.* **2012**, *22*, 585.